International Journal on Recent and Innovation Trends in Computing and Communication
ISSN: 2321-8169 Volume: 11 Issue: 9
***Article Received:** 25 July 2023 **Revised:** 12 September 2023 **Accepted:** 30 September 2023*

Machine Learning-Based Optimization Method for the Oxygen Evolution and Reduction Reaction of the High-Entropy Alloy Catalysts

Jagannath Jijaba Kadam[1*], Mahadeo Ramchandra Jadhav[2], Siddhanath Abasaheb Howal[3], Ganpati Martand Kharmate[4], Vikram Uttam Pandit[5]

[1*]Professor, Chemistry Department, Bharati Vidyapeeth college of Engineering, Navi Mumbai, India, Email: jjkadam702@gmail.com

[2] Assistant Professor, Chemistry Department, Bharati Vidyapeeth college of Engineering, Navi Mumbai, India, Email: mahadeojadhav2013@gmail.com

[3] Assistant Professor, Gharada Institute of Technology, A/P Lavel, khed, Ratnagiri, Maharashtra, India, Email: siddhu.howal@gmail.com

[4]Assistant Professor, Physics Department, Bharati Vidyapeeth college of Engineering, Navi Mumbai, India, Email: ganpati.kharmate@bvcoenm.edu.in

[5] Assistant Professor, Haribhai V. Desai College, Pune-411002, Maharashtra, India, Email:vikramupandit@gmail.com

Abstract: In recent times, high-entropy alloys (HEAs) have found application in heterogeneous catalysis, capitalizing on their vast chemical potential. Yet, this extensive chemical landscape presents significant challenges when attempting a comprehensive exploration of HEAs through traditional trial-and-error approaches. Therefore, the machine learning (ML) approach is offered to appearance into the catalytic activity (CA) of countless sensitive sites on HEA surfaces in the oxygen-lessening response (ORR) and oxygen evolution reactions (OER). In this research, a Density Functional Theory (DFT) with a supervised ML model is assembled and founded on the gradient boosting regression (GBR) algorithm that predicted the O2 adsorption energies with a high overpotential of all surface sites on the two HEAs. Initially, the HEAs Co-Fe-Ga-Ni-Zn and Al-Cu-Pd-Pt offer a framework for adjusting the composition of disordered multi-metallic alloys to regulate the activity and selectivity of the reduction of oxygen to extremely reduced compounds. This attains generalizability, high accuracy and simplicity with the proposed technique. For fine-tuning such features, HEAs provide a huge compositional space. Consequently, the research reports the custom of the Bayesian optimization model based on HEA active compositions to suppress the formation of Oxygen (O2) and with strong O2 adsorption to favour the lessening of O2. The GBR approach is applied to build a highly accurate, easily generalizable, and effective ML model. The proposed work is analysed using Python software. The findings show that the separate charities of correlated metal atoms close to the responsive site are mixed to form the adsorption energy, which is clear from a thorough analysis of the data. It is suggested that a highly effective HEA catalyst composed of Co-Fe-Ga-Ni-Zn and Al-Cu-Pd-Pt be exploited, which is an effective method for further enhancing the ORR CA of potential HEA catalysts. An instruction manual for the logical design and synthesis of HEA catalysts' nanostructures is provided by the proposed research.

Keywords: High-Entropy Alloys, Oxygen Reduction Reaction, Oxygen Evolution Reactions, Gradient Boosting Regression, Density Functional Theory, Bayesian Optimization.

I. INTRODUCTION

The current focus of advancement in materials chemistry research centers around the utilization of composite electrodes, rooted in atomic-level engineering and the control of multilayer structures. The primary area of study in the sphere of water splitting is the formation of inexpensive and effective electro catalysts. Hydrogen generation by water electrolysis is receiving increasing attention due to the benefits of good flexibility, high efficiency, and minimal production of carbonaceous species. Ere, several strategies such as changing the crystal structure and generating the microstructure are extensively employed to boost the inherent CA and double the number of vigorous positions in catalysts made of nonprecious metals. Particularly, the alloying of several elements into one phase could disclose peculiar physicochemical characteristics, including higher CA [1]. Effective sampling of catalyst materials has also advanced, and experimental catalyst development for a diversity of processes and constituent elements has actively utilised combinatorial investigation of vast alloy composition spaces [2]. Due to the close correlation between the conductivity and intrinsic activity of materials and the electrocatalytic performance, great efforts have been made to adjust electronic properties and design multilayer systems [3]. In the electrocatalytic water-splitting process, a very stable and inexpensive material is urgently needed for the OER, which is a vital step in both water-splitting systems and rechargeable metal-air batteries. [4, 5].

The OER determines the rate of energy conversion and also serves as a testing ground for the manufacture of integrated OER electrodes with high activity and high conductivity. However, there is still a significant obstacle to overcome in the formation of low-cost, highly effective OER electrocatalysts that can be applied industrially on a wide scale. Similarly, the

International Journal on Recent and Innovation Trends in Computing and Communication
ISSN: 2321-8169 Volume: 11 Issue: 9
***Article Received:** 25 July 2023 **Revised:** 12 September 2023 **Accepted:** 30 September 2023*

ORR is one example of a crucial response in the hydrogen cycle. The conception of affordable catalysts for the oxygen reduction process (ORR) has a significant influence on fuel cells in the direction of extremely effective low-emission energy conversion [6]. Contemporary compounds are quite far from perfect and cannot satisfy the requirements for manufacturing application that is economically feasible on a global scale. Further developments are therefore urgently needed to reach that end aim [2]. However, to close the gap between theoretical calculations and real necessary potentials, efficient catalysts are required due to the slow kinetics of the OER, particularly the enormous dynamic barrier caused by the four-step proton-coupled electron transfer process. Although the excellent efficiency of several noble metal-based materials as OER electrocatalysts has been established, their high cost and unavailability significantly hinder their widespread commercialization. Better catalysts can be produced by customising the HEA composition to increase the supply of these adsorption energies. This is helpful because, to fulfil the rising global energy demand and battle climate change, new substances are particularly wanted to enhance chemical processes for the conversion of supportable energy. This motivates research on OER electrocatalysts based on non-noble metals [7].

Chemically intricate catalytic materials have drawn a lot of consideration from researchers in the domains of materials science and engineering. It has been established that better qualities may be obtained for the custom of current catalytic materials in several significant applications, including wastewater cleanup, catalysis, energy storage, and fuel cells. Metallurgists have suggested a similar design strategy to increase the chemical complexity of alloys by synthesising multi-principal element alloys, commonly known as high entropy alloys (HEAs), for improved mechanical qualities. Some HEAs moreover display functional traits that are promising, such as super-paramagnetism and superconductivity [8]. HEAs, which combine five or additional rudiments into a solid-solution stage crystal with a steady fraternization entropy, have recently gained popularity as a brand-new class of catalytic materials. The routine of multimetal HEAs as catalysts for energy adaptation and water splitting, such as oxygen evolution processes, has been identified as a viable replacement for traditional noble metals and metal oxides [10]. HEAs are immensely developing as a new type of catalyst in the alloy industry with a distinctive microstructure and exceptional physicochemical and mechanical characteristics, which have produced an inordinate deal of attention worldwide [9, 10].

It has been suggested that combining several metals into an alloy might provide unanticipated physicochemical characteristics, such as higher tensile strength, CA and corrosion resistance. HEAs are a novel class of materials that are shaped by mixing five or additional rudiments in an alloy with equal or nearly equivalent molar percentages (HEAs) [11, 12]. HEA has received a ration of kindness recently and might offer solutions to the problem at hand [13]. ML techniques have been proven to efficiently search for the intended optimum and to discover patterns that people may supervise in the expanding chemical space where the structure-property connection grows more complicated [14, 15]. The rest of the work is organized as follows, section 2 reveals the literature survey of the work, section 3 portrays the research problem definition and motivation, and section 4 depicted the proposed research methodology. Accordingly, section 5 illustrates the experimentation and result from the discussion part, and section 6 demonstrates the research conclusion.

II. Literature Survey

Chemically intricate catalytic materials have drawn a portion of devotion from researchers in the provinces of materials science and engineering. Numerous enlightening and beneficial HEA practices and methodologies have been revealed in recent years. Though there have been roughly thorough reviews on the topic of HEA preparation, there is not much focus on the most recent HEA preparation methods for catalytic applications. To increase the ORR catalytic movement of talented HEA substances by optimising the HEA superficial construction, Wan *et al* [16] proposed an ML-assisted finding of extremely well-organized HEA catalysts. This recommendation makes custom of a highly efficient HEA catalyst.

The composition of HEAs can be varied greatly to optimise their catalytic characteristics. Such complex surfaces have a large amount of multi-element atomic surface sites, which help to provide a nearly continuous range of reaction intermediate adsorption energies that characterise CA. Fan et al [17] proposed HEA electro-catalytic electrode for alkaline glycerol valorization coupled with acidic hydrogen generation. With a low overpotential and a strong selectivity for format products, this approach confirmed attractive performance for GOR electrocatalysis.

Pt-based HEA nanoparticles were proposed by Chen *et al* [18] as functional electrocatalysts for hydrogen and oxygen evolution. ACS A bottom-up shear-assisted liquid metal superficial decrease technique is described for the manufacture of HEA nanoparticles at room temperature. An ML-aided optimization of HEA CA was suggested by Clausen *et al* [19]. This approach demonstrates the viability of unbiased in silico pre-screening and catalyst candidate development, which will allow us to overcome the previously intractable barrier of finding HEA catalysts. Computational methodology, which is openly accessible on GitHub, is intended to help other research teams rapidly find promising HEA catalysts. A HEA with Mo-Coordination was suggested by Mei *et al* [20] as an effective electrocatalyst for the OER. Discovery establishes a procedure for generating effective, economical OER electrocatalysts, which may speed up the development of OER catalysts.

Sharma *et al* [21] proposed a low-cost HEA for a high-efficiency oxygen evolution process. The technique is an affordable, simple, and scalable process for making nanocrystalline HEA materials for an OER investigation. Additionally, this research will contribute to a novel, high-performance, high-entropy OER electrocatalyst while improving the understanding of the mechanisms at the CFGNZ/electrolyte interface. This will help build OER catalysts that are more effective shortly. These results lend credence to the idea that the multi-component HEA made up of Co, Fe, Ga, Ni, and Zn components is a superb OER catalyst, with the making of metallic oxide serving as the active ingredient and is extremely important for the stability of CFGNZ alloy.

International Journal on Recent and Innovation Trends in Computing and Communication
ISSN: 2321-8169 Volume: 11 Issue: 9
***Article Received:** 25 July 2023 **Revised:** 12 September 2023 **Accepted:** 30 September 2023*

Li *et al* [22] proposed an oxygen evolution anode made of a single phase of the HEA (FeCoNiMnMo) working for more than a thousand hours in an alkaline solution. Mo is valuable for enhancing oxygen evolution performance; however, it dissolves readily in alkaline solutions. HEAs can prevent the dissolving of metals, although it is challenging to evenly dissolve the components with significant physical variations. Infinite OER candidates are available for effective water electrolysis due to the construction and enterprise of the single-phase HEA electrode.

HEA nanoparticles produced from polymetallic MOF were suggested by Wang *et al* [23] as potential electrocatalysts for the alkaline oxygen evolution process. Due to their distinct features, HEA-based materials have recently been intensive exploration as potential catalysts in water electrolysis. The manufacture of reliable, effective high entropy catalysts is still difficult. Here, a straightforward and scalable method for constructing enhanced HEA nanoparticles from the polymetallic metal-organic framework is disclosed. Face-centred cubic HEA is encased in a very thin carbon shell in the new core-shell nano-architectures. This work indicated the viability and benefit of using strong, long-lasting alloys with high entropy to catalyse the electrochemical water-splitting process.

HEA with Mo-Coordination as an Efficient Electrocatalyst for OER was proposed by Mei *et al* [24]. It is the most talented technique for storing and converting renewable energy is electrochemical hydrolytic hydrogen generation. The kinetic sluggish OER, however, restrains the anode's ability to electrolyze water. Modern OER catalysts are constrained by their high noble metal concentration and poor OER activity. This technique described a method for producing stable and effective HEA catalysts using molecular coordination. Zhang *et al* [25] proposed a method for constructing a metal (oxy) hydroxide surface on a HEA for serving as an electrocatalyst for the OER that participates in the lattice oxygen system. By building metal (oxy) hydroxides in situ on the high entropy FeCoNiAl alloy, a lattice-oxygen-contributed OER electrocatalyst was produced (HEA) [26- 29].

III. Research Problem Definition And Motivation

HEAs have been applied in the scope of catalysis because they have a large chemical space due to the tremendous variability of inherent surface and element mixtures complexity, which enables them to function as catalysts with greater activity, selectivity, and stability [30-33]. In numerous distinct processes, including the hydrogen evolution reaction (HER), ORR, carbon dioxide reduction reaction (CO2RR), and methanol oxidation, HEAs have so far been examined as highly effective catalysts [34-36]. These investigations have been primarily experimental. The lethargic kinetics of ORR and OER is a key issue which hinders the practical application of fuel cells and metal-O_2 batteries [37-38]. However, the slow OER typically calls for a significant over-potential [39-41]. A catalyst with high activity is required to speed up the OER's kinetics and lower the reaction over potential [42-44].

HEAs, which make custom of large chemical space, have lately been utilized in the range of heterogeneous catalysis. Huge chemical space, however, also poses formidable difficulties for the thorough investigation of HEAs using conventional trial-and-error methods [45-46]. The ORR CA of a huge quantity of oversensitive sites on HEA surfaces is thus investigated using the ML approach. The classic DFT method can be significantly outperformed computationally by the ML approach while still predicting CA with good accuracy [47-48]. Additionally, by illuminating the nonlinear link between a material's structure and properties, ML techniques can disclose the intrinsic description of catalytic reactions. For dissimilar kinds of batteries to be commercially successful, cost-efficient, high-activity, and stable bi-functional catalysts for oxygen reduction and evolution processes (ORR/OER) are a requirement. Consequently, the research motivates to present of the ML-based optimization technique for oxygen evolution and reduction.

IV. Proposed Research Methodology

The HEA's suitability as catalysts is influenced by a total of variables, including their elemental content, mode of production, and surface shape. High entropy electrocatalyst applications are hampered by the prevalent high overpotential caused by insufficient study and uncertain catalytic mechanisms of HEA electrocatalysts. Developing highly efficient catalysts for ORR and OER is crucial for water splitting and rechargeable metal-oxygen batteries. Therefore, the ML technique is proposed to examine the CA of loads of sensitive places on HEA surfaces in the ORR and OER. Co-Fe-Ga-Ni-Zn and Al-Cu-Pd-Pt are two examples of HEAs that may be employed as starting points to adjust the composition of disordered multi-metallic alloys to alter the efficiency and activity of the reduction of oxygen to significantly decreased compounds.

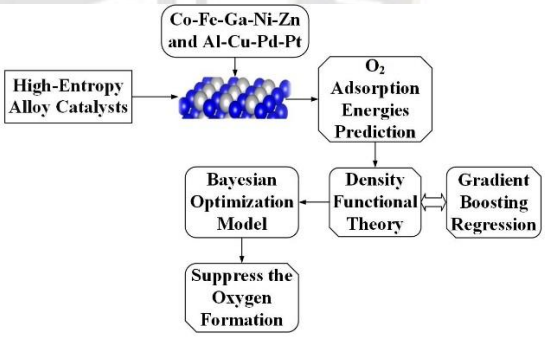

Figure 1. Block Diagram of the Proposed Work

The block diagram of the proposed work is presented in figure 1. The proposed work combining DFT with a supervised ML model is constructed based on the GBR algorithm that predicted the O_2 adsorption energies with a high overpotential of all surface sites on the two HEAs. This attains simplicity, generalizability, and high accuracy with the proposed technique. A large compositional space is provided by HEAs for adjusting these features. Consequently, the research reports the usage of the Bayesian optimization model based on HEA active compositions to suppress the formation of Oxygen (O_2) and with strong O_2 adsorption to favour the decrease of O_2. Increasing the chemical complexity of the catalyst is one technique to adjust the CA. Typically referred to as HEAs, these alloys contain five or further significant components in a single solid solution phase. For example, Schuhmann and coworkers

International Journal on Recent and Innovation Trends in Computing and Communication
ISSN: 2321-8169 Volume: 11 Issue: 9
***Article Received:** 25 July 2023 **Revised:** 12 September 2023 **Accepted:** 30 September 2023*

prepared Co-Fe-Ga-Ni-Zn and Al-Cu-Pd-Pt nanoparticles (NPs), produced by blasting these metals into an ionic liquid, showed electro CA for ORR and OER that was comparable to Pt/C.

A. High-Entropy Alloys

The composition space for (HEAs; also known as single-phase compositionally complicated solid solutions) is extremely broad, allowing for the optimisation of catalytic characteristics. A near-continuum of the reaction intermediate adsorption energies, which are indicative of CA, is produced by the numerous multi-element atomic surface sites present on such complex surfaces. The spreading of these adsorption energies can be enhanced by customising the HEA composition to provide better catalysts. This is advantageous because novel promoters are particularly desired to speed up chemical reactions for sustained energy conversion to satisfy the rising global energy demand and to stop climate change. The ORR is one example of a crucial reaction in the hydrogen cycle where current materials are still far from optimal and cannot match the requirements for economically feasible development implementation on a global scale. To achieve that final goal, more innovations are therefore urgently needed.

An effective sampling of catalyst materials has also advanced, and combinatorial exploration of enormous alloy structure spaces has been actively exploited as a technique in empirical catalyst development for a change of processes and constituent elements. However, when the assortment of constituent elements rises, the combinatorially enormous quantity of alternative compositions also expands, making it impossible to complete individual point testing in a reasonable amount of time (see Supporting Information (SI)). As a consequence, it becomes necessary to sample the composition space more effectively, perhaps by directing the search with the help of a surrogate function. For intelligent sampling issues, Bayesian optimisation of a Gaussian process is a workable solution. Bayesian optimisation has also been applied to improve the CA for methanol oxidation of ternary alloys. To ascertain whether such a search is tractable in the first place, it is essential to establish in advance many tests would be required in such a compositional search.

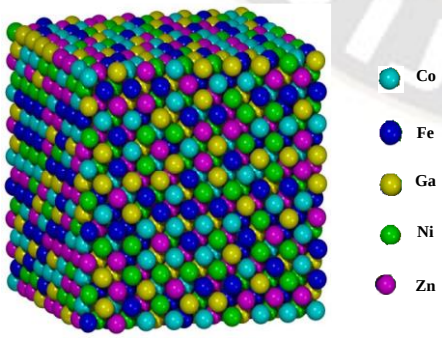

Figure 2. Geometric Structure of the HEA Catalyst

The geometric layout of the Co-Fe-Ga-Ni-Zn and Al-Cu-Pd-Pt HEA Catalyst is shown in figure 2. Few research have been done, therefore modelling of highly diverse and complex surfaces' CA is still in its infancy. Research is also being done on the modelling of other catalytically relevant characteristics, such as surface stability under reaction circumstances. We suggest a method to estimate the number of experimentations obligatory using a model that has been found to accurately forecast experimental trends for electrocatalytic ORR across hundreds of various alloy compositions within the Co-Fe-Ga-Ni-Zn and Al-Cu-Pd-Pt system. As a consequence, we anticipate the model to duplicate the difficulty of a similar experimental search and hence be adequate as a stand-in for simulating the majority of the required trials. Thus, the number of tests required for upcoming composition optimisations can be approximated by sampling alloy compositions from the model.

Utilising the Co-Fe-Ga-Ni-Zn and Al-Cu-Pd-Pt HEAs as model systems for composition optimisation, we propose alloy compositions for which high CA for the ORR are predicted using the kinetic perfect in conjunction with Bayesian optimisation. By doing this, one can obtain a sample of as few compositions as possible, and the estimated quantity of research essential to find activity maxima is obtained. The estimated optima are then put through an experimental validation process. Additionally, it is likely to verify with some degree of assurance that all local and global optimal compositions have been identified by the Bayesian optimisation by selecting the entire interplanetary of alloy arrangements with the model, for instance, in 5-atomic percent (%) intervals.

1. Density Functional Theory (DFT) Method

The theoretical investigation of the catalytic performance of all the sites using simply the conventional DFT method is greatly complicated by the millions of various active-site settings of HEAs and the existing restricted computational implementation capability. Finding new techniques or improving existing ones can significantly lower the overall computational cost, making this among the most plausible approaches for overcoming the processing power limit. Because it is so beneficial in these two areas, ML is drawing attention from all across the world. The ML approach can predict catalytic activities with excellent accuracy while drastically cutting the computational cost compared to the conventional DFT method. Additionally, by illuminating the nonlinear link between a material's structure and properties, ML techniques can disclose the intrinsic description of catalytic reactions. The cutting-edge ML-assisted theoretical computations method is now a rising star in the catalysis industry as a result.

When compared to the full experimental materials screening, this combination of ML and DFT can significantly lower the charge of resource discovery. For ML, however, only the costly screening via high-throughput experiments would suffice. It has been claimed that binary systems successfully make routine of the periodic DFT to calculate both the ΔE_f and the structural information of a system. However, to concept, the HEA, numerous potential atomic configurations essential to be hypothesised and confirmed through thermodynamically advantageous structures.

Even though all information can be collected, the routine computation using DFT alone would be time-consuming. However, the stability of some quandary HEA kinds was initially examined in this work. Then, the relationship between O* fascination vitalities and the ORR volcano curvature corresponding to the ORR CA of reactive locations on HEA

International Journal on Recent and Innovation Trends in Computing and Communication
ISSN: 2321-8169 Volume: 11 Issue: 9
***Article Received:** 25 July 2023 **Revised:** 12 September 2023 **Accepted:** 30 September 2023*

surfaces was developed. To estimate the O* captivation serves of masses of mercurial situates on various crystal facets of HEAs with high accuracy, an excellent ML model was built through suitable feature engineering, data extraction, and model validation techniques. To identify highly effective HEA catalysts and identify the source of their ORR activity, additional analysis of the expected findings and the ML models was performed.

The details of the DFT scheming and ML forecast model can be founded in the following SI. The ΔE_f of Co-Fe-Ga-Ni-Zn and Al-Cu-Pd-Pt-based HEAs can be calculated as equation (1).

The following SI may be applied to establish the specifics of the DFT calculation and ML prediction model. Al-Cu-Pd-Pt and Co-Fe-Ga-Ni-Zn-based HEAs' ΔE_f can be computed using equation (1).

$$\Delta E_f = E_{total}^{HEA}(CoFeGaNiZN\_\text{AlCuPdPt}) - \sum_i (c_i E_{total}^{element}) \quad (1)$$

Where $E_{total}^{element}$ the total energy for each element is determined from its natural form and $E_{total}^{HEA}(CoFeGaNiZN\_\text{AlCuPdPt})$ is the total energy for the HEA system.The c_i is the element concentration.

In identical supercells and using the same DFT parameters, the energy of the reference molecules CO and O_2 in the gas phase was estimated. The predicted adsorption energies for O and CO are

$$\Delta E_{*CO} = E_{*CO} - E_* - E_{CO}$$
$$\Delta E_{O^*} = E_{O^*} - E_* - \frac{1}{2}E_{O_2}$$

Where ΔE_{*CO} and ΔE_{O^*} are the adsorption energies of CO and O, respectively; E_{*CO} and E_{O^*} are the relaxed DFT energies with the adsorbate; E_* is the DFT energy of the slab without any adsorbate; and E_{CO} and E_{O_2} are the references' molecular gas phase DFT energies. The DFT-calculated framework parameters of the constituent elements in the slab's top layer were preferred as the weighted average for the matrix stricture. The consequence of strain on a genuine HEA surface should be most precisely accounted for by this CA.

2. Gradient Boosting Regression

The GBR is among the most challenging models to optimise because of the numerous hyper-parameters involved. The ensemble method and the individual learners each have their own sets of parameters, which is due to the boosting algorithm in GBR and the cause of this complexity. The ideal hyper-parameters are configured to employ a learning rate of 0.125, a loss of LAD, a mass tree depth of 5, a minimum sample size per leaf of 2, a minimum sample split of 0, and 500 estimators. Once the best model has been selected, the feed-forward time is about the same as it is for the other two algorithms.

The model's convergence speed is governed by the learning rate. Thus, a learning rate that is too high could cause the model to converge on a local minimum rather than the ideal solution, whereas a rate that is too low would prevent convergence altogether. Hyper-parameters for the GBR and those for the regression trees are tuned in addition to the hyper-parameters defining the GBR. A grid search between 0.07 and 0.125 was applied to optimise the learning rate. During this grid search, a model was incrementally built and evaluated for parameter values that fell within the predetermined range, allowing for optimal learning rate tuning. Here, GBR makes a model in a forward, stage-wise manner, allowing for optimisation on any loss function that can be differentiated.

ML Process

Although the adsorption energies of the masses of combative sites on HEA may be calculated using the volcano bend, it is nearly impossible to bridge the CA and the adsorption energies of O*. It is now imaginable to ascertain the activity of millions of sites on HEAs appreciations to the introduction of ML, which links the local nuclear situation surrounding the sites with the adsorbate strength. For the initial dataset for generating ML models, 360 volatile sites on HEAs with various Miller index outsides and constituent rudiments were elect at random. DFT simulations were then used to determine the fascination dynamism of OH* radicals on these sites.

The first necessary condition before any ML-based prediction is the identification and categorization of materials, or mapping them according to their characteristics (descriptors), which could be accomplished using ML classification models. For the categorization of the electrocatalyst, ML algorithms are exploited. Additionally, we made an effort to categorise product categories by grouping every potential product into two or three different, larger groups. Four ensembles of ML algorithms were assessed to examine the predictability of various models for locating missing data. The O_2 reduction responses training data were utilized to train the algorithm. After that, the algorithms were put into practice to forecast the test dataset's faradic efficiency, applied potential (AP), and present density. Automatic hyper-parameter tuning is done with the help of the ML hyper-parameter optimisation module.

Each classification method is assessed using its accuracy score (%), which is calculated as the proportion of correct predictions to all other predictions. Several statistical measures, including the mean squared errors (MSE) and the root, means squared errors (RMSE), were employed to assess each ML algorithm's performance for prediction.

$$MSE(y, \hat{y}) = \frac{1}{n}\sum_{i=0}^{n-1}(y_i - \hat{y}_i)^2 \quad (2)$$

$$RMSE(y, \hat{y}) = \sqrt{\frac{1}{n}\sum_{i=0}^{n-1}(y_i - \hat{y}_i)^2} \quad (3)$$

Where y_i and $\hat{y}_i$ stand for the true and expected standards, respectively, and n denotes the sample size. Metallic, non-metallic, and chemical catalysts are the three primary categories into which O_2 electrocatalyst materials are commonly divided in the predictive algorithm. The physicochemical and electrocatalytic possessions of each group of electrocatalyst materials vary. The efficiency of an electrocatalyst material may therefore be constrained and limited to the category of catalyst materials to which it belongs. Here, classify various electrocatalyst materials into multiple categories based on their performance using an ML classification model.

3. Bayesian Optimization

Bayesian optimisation was exploited to select the samples for the inquiry. A technology that enables a guided search in an uncharted multidimensional space is Bayesian optimisation. As a result, it may be utilized in conjunction with trials to find a catalyst with the best activity speedily. This optimisation is utilised in this study to identify the Co-Fe-Ga-Ni-Zn and Al-Cu-

International Journal on Recent and Innovation Trends in Computing and Communication
ISSN: 2321-8169 Volume: 11 Issue: 9
***Article Received:** 25 July 2023 **Revised:** 12 September 2023 **Accepted:** 30 September 2023*

Pd-Pt component that is most conducive to the oxygen oxidation reaction. The random forest regression framework that was developed on the experimental information was used in conjunction with the Bayesian optimisation to generate a diversity of ideas for additional research. It is crucial to first think about which parameters will be utilised as the parameters for the input and output before building this regression.

A quantitative estimate of the oxygen oxidation affinity necessity be the output parameter of the equation because the goal of this research is to identify the best catalyst. The oxygen oxidation onset potential will be utilized to further examine this indicator of oxygen oxidation affinity. By placing a monolayer of oxygen on top of the nanoparticle, which was then oxidised by an anodic sweep in an H_2-rich atmosphere, the oxygen oxidation onset potential was determined electrochemically. As a probe reaction to increase the potential at which the oxygen monolayer was oxidised, the hydrogen oxidation reaction (HOR) was exploited. When an increase of 1.5 mA mg^{-1} Co-Fe-Ga-Ni-Zn and Al-Cu-Pd-Pt over the capacitive current was detected, this was the point at which oxygen oxidation was determined. The machine-learning models only considered catalysts that were active for the HOR beyond the oxygen oxidation start potential since the oxygen oxidation was examined using the HOR as a probe reaction.

The model's input parameters ought to take into account the HEA's characteristics that affect the activity of oxygen oxidation. The HEA's chemical makeup, which is the most obvious option in this case, is its elemental makeup. It is impossible to systematically and swiftly evaluate the final composition of the manufactured nanomaterials. A specific Co-Fe-Ga-Ni-Zn and Al-Cu-Pd-Pt particle's composition can be characterised by a numeral of different parameters, although the proportion of each precious metal utilised during synthesis is likely the most tightly controlled. Input parameters were therefore based on the metals employed in the synthesis. All models will be identified with the term "synthesis models" if the synthesis precursor ratio was utilised as an input.

The predicted improvement acquisition function (4) was utilised for the Bayesian optimisation.

$$[I(r)] = \int_{-\infty}^{y_{min}} (y_{min} - y)(y; \mu, \sigma) dy = (y_{min} - \mu)\Phi\left(\frac{y_{min}-\mu}{\sigma}\right) + \sigma\Phi\left(\frac{y_{min}-\mu}{\sigma}\right) \quad (4)$$

Here, $I(r)$ the improvement function at a point r, y_{min} is the lowest current sampled so far in the optimization, y is the current being integrated over, N is the normal distribution function, the mean of which, μ is the Gaussian process predicted current at the point r, and whose standard deviation σ is the uncertainty predicted by the Gaussian process, Φ is the cumulative delivery function of the standard usual supply, and φ is the standard normal distribution function (i.e. with $\mu = 0$ and $\sigma = 1$).

Figure 3 shows the flow diagram of the algorithm for Bayesian optimisation. The surrogate function was started with two randomly selected compositions. The following composition to be investigated was then suggested using the predicted improvement acquisition function. The anticipated improvement accounts for both the surrogate function's existing density projections and the easily accessible prediction uncertainty. For more information on the implementation, see the SI. It is a common option and a frequently used acquisition function, making it a logical starting point for the current investigation. Equations (5)–(7) of the kinetic classical were then utilised to calculate the CA of the selected composition and Bayesian inference was then employed to update the procedure.

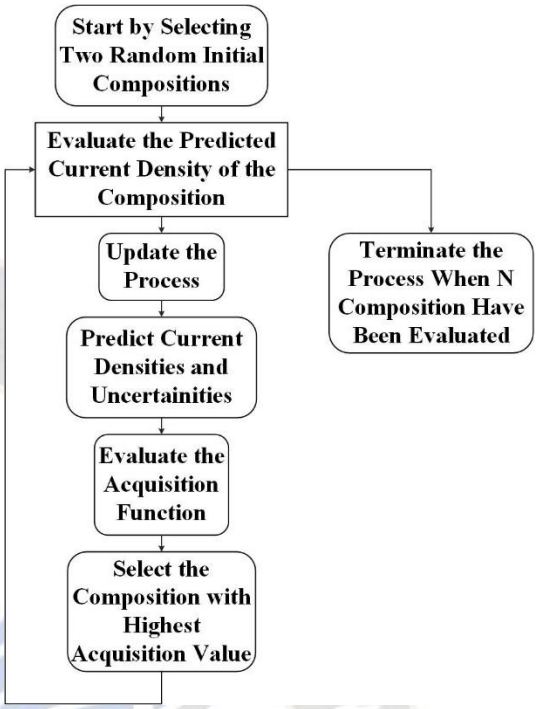

Figure 3. Flow Diagram of Bayesian Optimization Algorithm

Repeating this procedure allowed us to let the updated acquisition function select the following composition of interest, and in most cases, 150 iterations of the optimisation were sufficient to find the compositions that were the greatest vigorous locally optimal compositions.

$$j = \frac{1}{N}\sum_i^{N_{ads}} j_i \quad (5)$$

$$\frac{1}{j_i} = \frac{1}{j_D} + \frac{1}{j_{k,i}} \quad (6)$$

$$j_{k,i} = -exp\left(-\frac{|\Delta G_i - \Delta G_{opt}| - 0.86eV + eU}{k_B T}\right) \quad (7)$$

Here, N is the number of surface atoms in the modelled surface, j is the per-site recent density (in arbitrary units solely used for evaluating CA among compositions), and N_{ads} is the quantity of sites at which adsorption has occurred. (after considering the intersite neighbour blocking), j_i is the current at surface site i modelled using the Koutecky– Levich equation, j_D is the Diffusion-limited current (with a value of -1) limits the current at each site to sigmoidal increases only at large overpotentials, volcano relationship with the adsorption energies, ΔG_i i$j_{k,i}$ is the kinetically limiting current for site i modelled using an Arrhenius-like expression assuming a Sabatier s the *CO or O* adsorption free energy, ΔG_{opt} is the optimal *CO or O* adsorption free energy (set to 0.1 eV and 0.2 eV larger than for $Pt(111)$ for *CO and O* respectively as suggested by theory and experiment), e is the elementary charge, U_{RHE} is the applied potential vs. RHE, k_B is the Boltzmann constant, and T is the total infection (set to 300 K).

International Journal on Recent and Innovation Trends in Computing and Communication
ISSN: 2321-8169 Volume: 11 Issue: 9
***Article Received:** 25 July 2023 **Revised:** 12 September 2023 **Accepted:** 30 September 2023*

V. Experimentation And Result Discussion

The constituent constituents of quinary HEAs are Co-Fe-Ga-Ni-Zn and Al-Cu-Pd-Pt, among other transition metal (TM) elements. They can build several HEA kinds. These elements were select because they share the same crystal structure, have a comparable atomic radius, and have a similar lattice constant. As a result, nanoparticles greater than 100 nm in size were produced. As a result, during catalytic measurements, they are not anticipated to exhibit particle-size effects. The intention behind choosing the precursor combinations was to construct an unchanging network of examples in a structured space that could be continuously expanded. These substances were elected because they have the same face-centred cubic (FCC) crystal structure, identical atomic radii, and close lattice constants. Additionally, it has been noted that the corresponding elemental metals are very effective ORR catalysts. Nine selected elements have fcc structures for the most part, therefore the HEAs of FCC are constructed to be studied in this work. Figure 2 depicts the assembled HEA Co-Fe-Ga-Ni-Zn and Al-Cu-Pd-Pt supercell, which has 256 atoms. Numerous HEAs with the same structure as the one mentioned above have been synthesised and have encouraging catalytic activity. As a result, Python software is used to analyse the planned work.

Table I. Table of System Configuration for Simulation

Simulation System Configuration	
Python Jupiter	Version 3.8.0
Operation System	Ubuntu
Memory Capacity	4GB DDR3
Processor	Intel Core i5 @ 3.5GHz
Simulation Time	50 seconds

Using Python software at version 3.8.0, the suggested methods are examined. The suggested work runs on the Ubuntu operating system and has 4GB of DDR3 memory. These specifics are shown in table 1 together with other information, such as the implemented work's processor being an Intel Core i5 @ 3.5 GHz and the duration of the simulation being 50 seconds.

The success of the *CO and O* adsorption energies in representing the catalytic reaction for the ORR via the associative mechanism is, thus, the foundation for this kinetic prototypical. When the potential is greater than 0.8 V vs. RHE, the dissociative mechanism, in which O_2 separates on the catalyst surface, will not contribute to the contemporary density. To enable predictions of *CO and O* adsorption energies on any surface site of the alloy at any composition, thousands of *CO and O* adsorption energies were computed using DFT for the model's design (for further information, see SI). Focusing on the *OH and O* intermediates is adequate to predict the CA because of the linear scaling between the adsorption energies of *OC and O*.

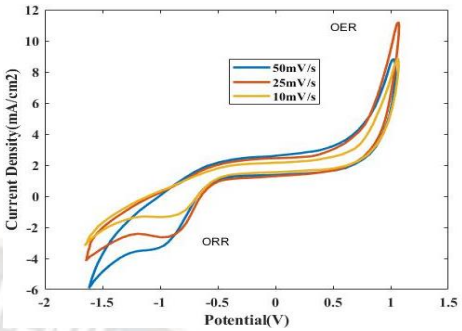

Figure 4. Electrochemical OER/ORR Properties

Figure 4 depicts the electrochemical properties of Co-Fe-Ga-Ni-Zn and 0.5 M, Al-Cu-Pd-Pt nanocomposites studied for their bifunctional CA (OER/ORR). Initially, the measurements were carried out to check the bi-functional electro-catalytic behaviour of Co-Fe-Ga-Ni-Zn and Al-Cu-Pd-Pt alloys at different scan rates (i.e. 10, 25 and 50 mV/s) under the applied potential range from -1 to +1 V as shown in the figure.

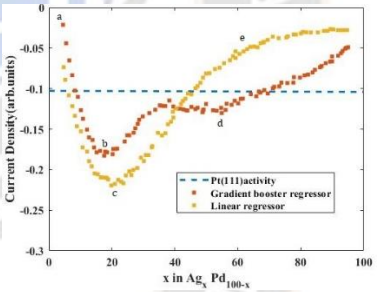

Figure 5. Simulated Current Densities

Figure 5 depicted the simulated current densities of the proposed work. When the anticipated existing density for the second alloy gradient-boosted model is compared to the identical findings from the linear model developed on the quinary alloys at high Pd content, both models indicate maximum inactivity.

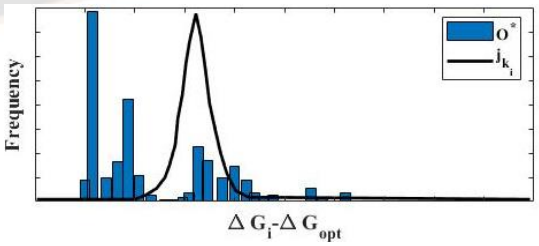

(a) Gradient-Boosted Model Trained Graph

International Journal on Recent and Innovation Trends in Computing and Communication
ISSN: 2321-8169 Volume: 11 Issue: 9
***Article Received:** 25 July 2023 **Revised:** 12 September 2023 **Accepted:** 30 September 2023*

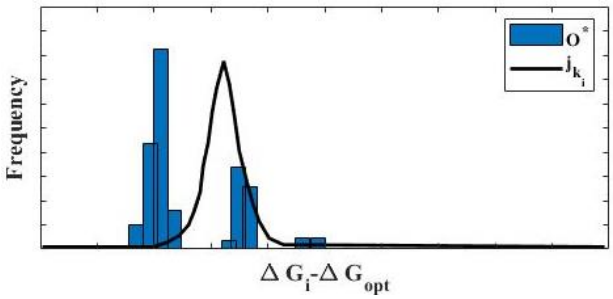

(b) Linear regression model trained Graph

Figure 6. Trained Regression Model on GFT

Figure 6 depicted the trained regression model on DFT-calculated samples. Except for a few three-fold Pd sites, as seen in figure 6(a) and (b), this activity is virtually entirely derived from O* bound in FCC hollow sites made up of two Pd atoms. The binary-trained model, in contrast to the quinary-trained model, maintains strong CA for a larger range of compositions, dropping below the activity of Pt (111) at about 45% due to the disparity of the model's Q prediction at on-top Pd sites. For Pd-Pt at the equimolar composition, we would therefore continue to anticipate a significant CA using the two alloy model.

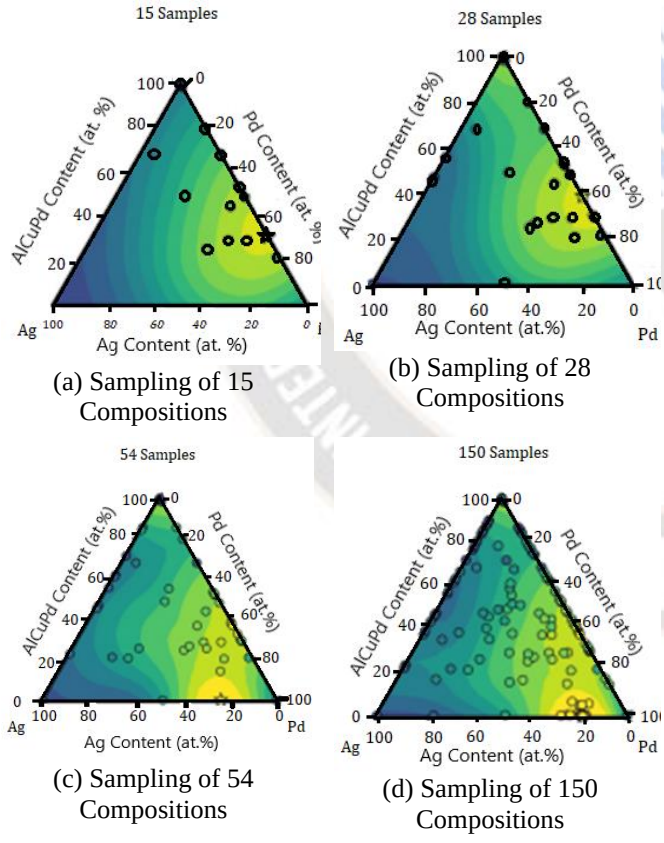

(a) Sampling of 15 Compositions

(b) Sampling of 28 Compositions

(c) Sampling of 54 Compositions

(d) Sampling of 150 Compositions

Figure 7. Pseudo-Ternary Plots of the Surrogate Function

Figure 7 shows the pseudo-ternary plots of the surrogate function following sampling 15, 28, 54, and 150 compositions (with Al, Cu, and Pd mutual into a single concentration). Blue and yellow colours denote regions with appropriately low absolute values of predicted modern density and high absolute values, respectively. The same locations in the diagram will invariably be occupied by greater compositions when the present densities across the quinary to the pseudo-ternary composition space are projected. The maximum absolute amount of the present density for overlapping compositions has thus been represented in the charts that are displayed. To be more precise, the present density is anticipated to fluctuate at relatively low frequencies, as evidenced by the length scale of roughly 0.4 that was discovered, which is disproportionately big in comparison to the molar fractions with values between 0 and 1. This is also validated by the surrogate function's outlines, which are observed to slowly alter as the molar fractions change in the figure. This implies that only a small quantity of native optima is anticipated for this hypersurface, which will probably result in fewer samples being required for their detection.

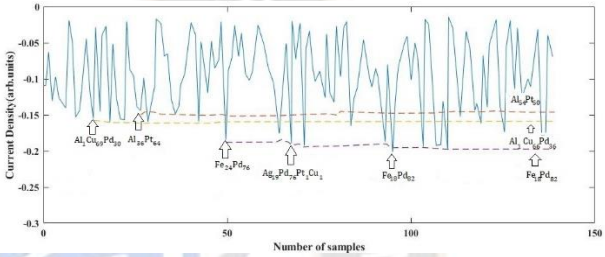

Figure 8. Current Densities Sampled during the Bayesian Optimization

Figure 8 displays several notable minima (i.e. compositions that have elevated absolute values of modelled current densities) that are sampled throughout an optimisation run, in addition to the appearance of the local minima of the surrogate value.

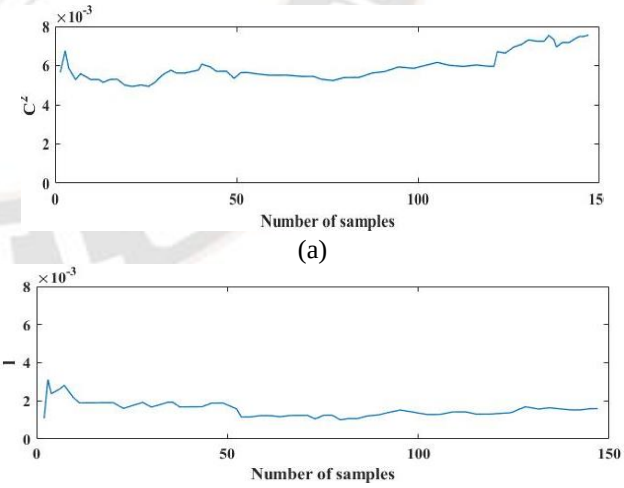

(a)

(b)

Figure 9. Figure for Length Scale and Hyper-Parameter for Number of Samples

The evolution of the value of the constant and length scale hyper parameters as more compositions are collected is depicted in figure 9(a) and (b). It's important to take note of the kernel's

International Journal on Recent and Innovation Trends in Computing and Communication
ISSN: 2321-8169 Volume: 11 Issue: 9
***Article Received:** 25 July 2023 **Revised:** 12 September 2023 **Accepted:** 30 September 2023*

length scale, which, while not directly applicable to compositions, does display how frequently the present density is anticipated to vary with composition. To be more precise, the existing density is anticipated to fluctuate at relatively low frequencies, as evidenced by the length scale of roughly 0.4 that was discovered, which is disproportionately big in comparison to the molar fractions with ranges between 0 and 1.

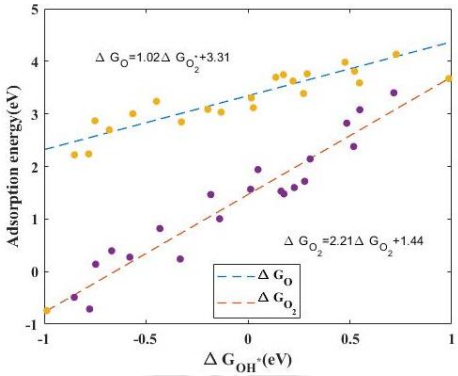

Figure 10. Scaling Relations between the Adsorption Energies of Reaction Intermediates

As mentioned above, the data shown in figure 10 indicate that there are apparent scaling links between the oxygen adsorption energies on HEA surfaces. The relationship between ΔG_{O*} and ΔG_{OH*} can be stated as $\Delta G_{O_2} = 2.21 * \Delta G_{OH*} + 1.44$, with a high coefficient of determination (R^2) of 0.91, in contrast to $\Delta G_{O*} = 1.02 *= 1.02 * \Delta G_{OH*} + 3.31$, with an R^2 of 0.85 for ΔG_{O*} and ΔG_{OH*}.

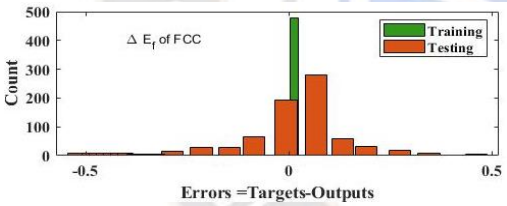

(a)

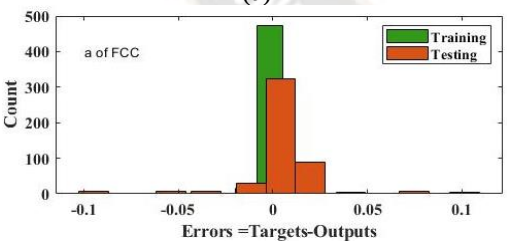

(b)

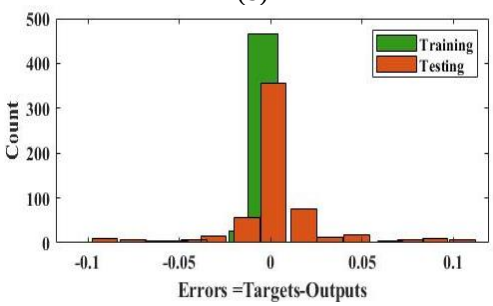

(c)

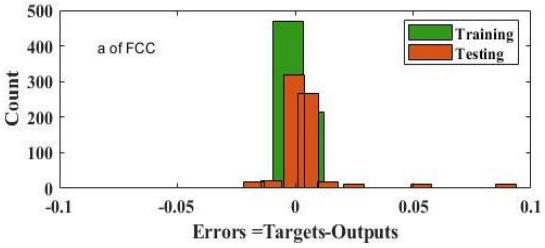

(d)

Figure 11. Results for Error Distribution

Figure 11 depicted the error distribution graph for the proposed work. Here, figures (a) and (b) revealed the error values in the testing were $\pm 0.5 KJ/mol^* f.u$ for $\Delta E_f(FCC)$ and $\pm 1.0 KJ/mol^* f.u$ for $\Delta E_f(BCC)$. Due to the strong association between features and error values in figures (c) and (d), the error values appeared to be closer to zero and more accurate than the ΔE_f.

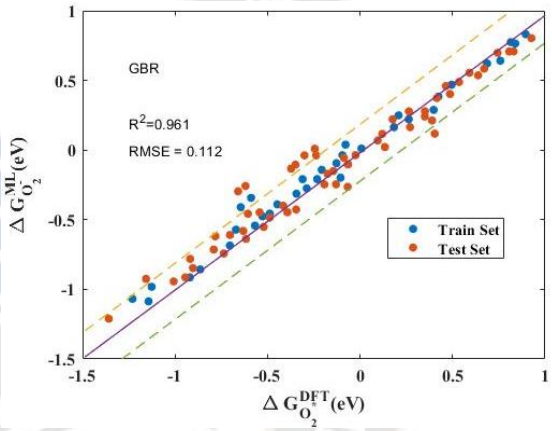

Figure 12. Parity Plot of DFT

Figure 12 depicts the parity plot of the GBR model compared to the entire dataset, and the GBR projected interest drives are in agreement with the DFT calculated energies. Indicating that the effective-trained GBR model attains great accuracy in prediction by learning significant details about the underlying pattern of the surrounding environment and adsorbate strength on HEA surfaces, closely all of the dots fell within the ±0.2 eV deviation range.

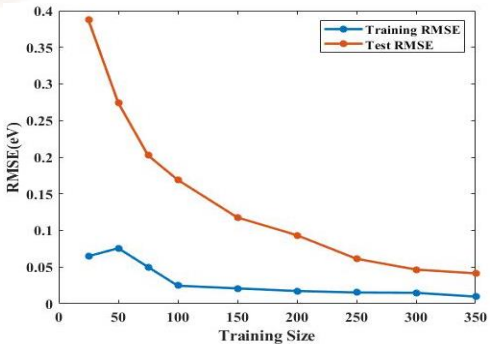

Figure 13. Learning Curve of the GBR Mode

International Journal on Recent and Innovation Trends in Computing and Communication
ISSN: 2321-8169 Volume: 11 Issue: 9
***Article Received:** 25 July 2023 **Revised:** 12 September 2023 **Accepted:** 30 September 2023*

The learning curve of the GBR model was plotted in figure 13. The figure depicted the learning curve of the GBR model with the training and testing RMSE, As the RMSE on the train and evaluation set continuously decreased as the training size increased and the convergent estimates were close to one another, it shows that there was no danger of overfitting.

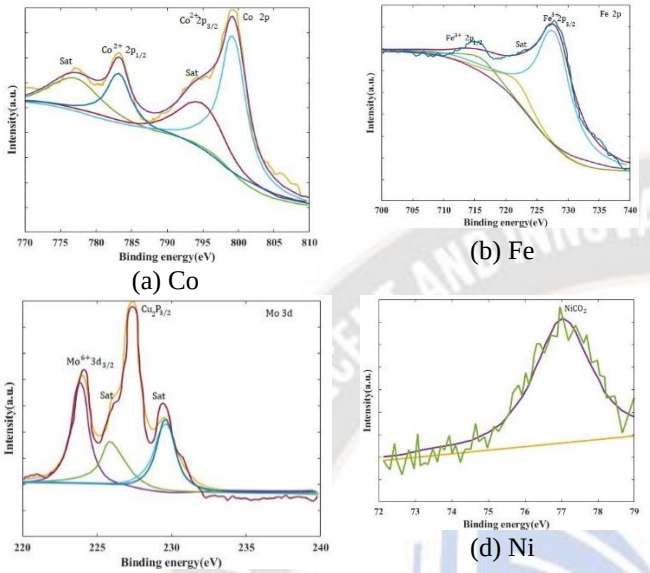

Figure 14. High-Resolution XPS Spectra of Co, Fe, Mo, and Ni

Figure 14 illustrates the results of an XPS measurement analysis of the $NiCO_2$- nanocomposites' surface composition. $NiCO_2$-NRs are supported by RGO sheets, as evidenced by the emergence of four peaks of Co, Fe, Mo, and $NiCO_2$ at ~800, ~728, ~240 and ~80 eV, respectively. Figure (a) shows three de-convoluted peaks that are connected to the Co high-resolution XPS spectra. Figure (b) displays bands at ~725 and ~735 eV of $Fe^{3+}2P$, respectively, from the High-resolution XPS spectrum of Fe3+2P. Mo's high-resolution XPS spectra are depicted in figure (c), which reveals two de-convoluted peaks at ~225 and ~228 eV. Figure (d) illustrates the NiCO2 high-resolution XPS spectra, which exhibit two major bands with energies of ~856 and ~875 eV of Ni 2p3/2 and Ni 2p1/2, respectively.

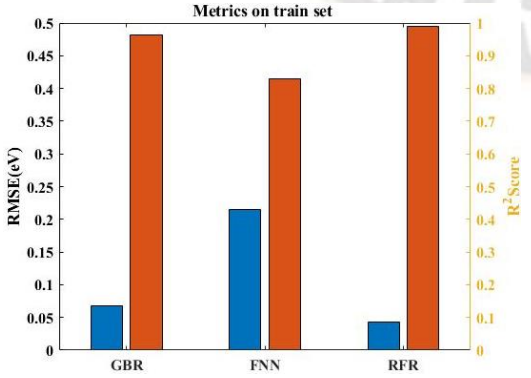

Figure 15. Comparison Graph of the RMSE for Training Set

Figure 15 illustrates the effects of model testing and training. Figure 12 illustrates the RFR and GBR models both behaved admirably on the train set despite a lower RMSE (0.1 eV) and higher R^2 score (0.95). The average metrics from the 500-time repetitive 4-fold cross-validation on the train and test set were similar, indicating minimal overfitting risk. Furthermore, the two models' error bars were rather brief, which indicated strong model robustness. Regarding the well-known FNN model, the model's performance was poor and the error bar was lengthy, demonstrating the FNN model's erratic nature.

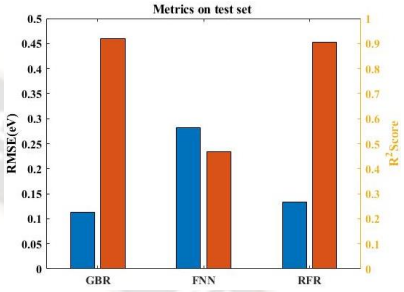

Figure 16. Comparison Graph of the RMSE for Testing Test

Figure 16 depicted the comparison graph for RMSE for the testing set. The proposed GBR model is compared with the existing FNN and RFR models. The small original dataset from DFT computations and the challenging hyperparameter tweaking procedure resulted in the FNN model's subpar accuracy. The metrics on the test set for the well-performing GBR and RFR models showed that the GBR model had a lower RMSE (0.112 eV) and a higher R^2 score (0.961) than RFR (RMSE of 0.129 eV and R^2 of 0.948). As a result, the ORR catalytic processes at sensitive sites on HEA surfaces and the fundamental structure of the native atomic environment may both be precisely described by the GBR model, which is the best ML model in this regard.

VI. Research Conclusion

HEAs are multi-principal component alloys that comprise five or other essentials, each close to equimolar proportion, and are frequently the complicated solid solution. In this study, with the help of ML, the potential of extremely active ORR electrocatalysts of various quinary HEA types was examined, taking into account the fact that the HEA surface can offer a near-continuum of oxygen between adsorption energies the distribution because of their enormous configurational and biological space. By using judicious model validation processes, feature engineering, and data extraction model validation processes, a well-performing GBR model with high accuracy, simplification and was formed. Masses of responsive sites on HEA surfaces with various coordination configurations, which are not amenable to analysis by conventional DFT calculations or experiments, can be accurately predicted using this superb GBR model. The adsorption energy on HEA surfaces is roughly a mixture of the different assistances of the metal atoms close to the mercurial site, as shown by the ML-predicted results and additional model analysis.

The suggested work is contrasted with the current FNN and RFR model, and it can be shown from the findings that the

suggested approach performs better than the other methods that are already in use. The model can predict the quantity of investigates prerequisites to find the best compositions in the enormous compositional space of quinary alloy systems while simultaneously suggesting the best alloy catalysts. The integer of experimentations essential to find the two quinary HEAs under study's most significant optima using the Bayesian optimisation of the kinetic classic applied here is around 50. The work is analysed using Python software. XPS measurement was carried out for the appearance of four peaks of Co, Fe, Mo, and $NiCO_2$ at ~800, ~728, ~240 and ~80 eV, respectively. However, the relationship between ΔG_{O*} and ΔG_{OH*} can be expressed as $\Delta G_{O_2} = 2.21 * \Delta G_{OH*} + 1.44$, with a high coefficient of determination (R^2) of 0.91. Accordingly, the planned method is associated with the existing FNN and RFR models, while compare to these methods, the proposed higher performance. However, the DFT-ML scheme shows that it has the aptitude and potential to lead the area of HEA catalysis because it can successfully navigate the extremely wide configurational and chemical space and provide a clear, concise roadmap for the practical synthesis of highly effective HEA catalyst nanostructures.

REFERENCES

[1] R. Wei, K. Zhang, P. Zhao, Y. An, C. Tang, C. Chen, X. Li, X. Ma, Y. Ma, and X. Hao, "Defect-rich FeCoNiPB/(FeCoNi) 3O4-x high-entropy composite nanoparticles for oxygen evolution reaction: Impact of surface activation," Applied Surface Science, vol. 549, pp.149327, 2021.

[2] J.K. Pedersen, C.M. Clausen, O.A. Krysiak, B. Xiao, T.A. Batchelor, T. Löffler, V.A. Mints, L. Banko, M. Arenz, A. Savan, and W. Schuhmann, "Bayesian Optimization of High-Entropy Alloy Compositions for Electrocatalytic Oxygen Reduction," Angewandte Chemie, vol. 133, no. 45, pp.24346-24354, 2021.

[3] Z.J. Chen, T. Zhang, X.Y. Gao, Y.J. Huang, X.H. Qin, Y.F. Wang, K. Zhao, X. Peng, C. Zhang, L. Liu, and M.H. Zeng, "Engineering microdomains of oxides in high-entropy alloy electrodes toward efficient oxygen evolution," Advanced Materials, vol. 33, no. 33, pp.2101845, 2021.

[4] S.A. Vajiha Begum, M. Pushpa Rani, "Recognition of neurodegenerative diseases with gait patterns using double feature extraction methods," IEEE - 2020 4th International Conference on Intelligent Computing and Control Systems (ICICCS), pp. 332-338, 2020, 10.1109/ICICCS48265.2020.9120920

[5] Nihar Ranjan Kar, "Osmotically Controlled Drug Delivery Systems: A Review," Indian Journal of Natural Sciences, vol. 13, no. 72, pp. 43372-43394, 2022

[6] H.J. Qiu, G. Fang, J. Gao, Y. Wen, J. Lv, H. Li, G. Xie, X. Liu, and S. Sun, "Noble metal-free nanoporous high-entropy alloys as highly efficient electrocatalysts for oxygen evolution reaction," ACS Materials Letters, vol. 1, no. 5, pp.526-533, 2019.

[7] L. Sharma, N. Kumar, R. Das, K. Tiwari, C.S. Tiwary, K. Biswas, and A. Halder, "Low Cost, Easy Scalable High Entropy Alloy (HEA) FeCoNiZnGa for High-Efficiency Oxygen Evolution Reaction (OER)," 2020.

[8] W.A. Saidi, "Optimizing the catalytic activity of Pd-based multinary alloys toward oxygen reduction reaction," The Journal of Physical Chemistry Letters, vol. 13(4), pp.1042-1048, 2022.

[9] Athi sakthi, Pushpa Rani, "Detection of Movement Disorders Using Multi SVM," Global Journal of Computer Science and Technology, vol. 13, no.1, pp. 23-25, 2013.

[10] Nihar Ranjan Kar, "Nanotechnology-Based Targeted Drug Delivery Systems for Brain Tumors," Indian Journal of Natural Sciences, vol. 12, no. 68, pp. 35081-35094, 2021.

[11] Q. Kang, D. Lai, W. Tang, Q. Lu, and F. Gao, "Intrinsic activity modulation and structural design of NiFe alloy catalysts for an efficient oxygen evolution reaction," Chemical Science, vol. 12, no. 11, pp.3818-3835, 2021.

[12] Z. Ding, J. Bian, S. Shuang, X. Liu, Y. Hu, C. Sun, and Y. Yang, "High entropy intermetallic–oxide core–shell nanostructure as superb oxygen evolution reaction catalyst," Advanced Sustainable Systems, vol. 4, no. 5, pp.1900105, 2020.

[13] J. Tang, J.L. Xu, Z.G. Ye, X.B. Li, and J.M. Luo, "Microwave sintered porous CoCrFeNiMo high entropy alloy as an efficient electrocatalyst for alkaline oxygen evolution reaction," Journal of Materials Science & Technology, vol. 79, pp.171-177, 2021.

[14] A. Komathi, M. Pushpa Rani, "Trust performance of AODV, DSR and DSDV in wireless sensor networks," IEEE - Second International Conference on Current Trends In Engineering and Technology," pp. 423-425, 2014.

[15] Nihar Ranjan Kar, "Liposomal Drug Delivery System: An Overview," Shodhasamhita: Journal of Fundamental & Comparative Research, vol. VIII, no. 5, pp. 123-134, 2022.

[16] N.K. Katiyar, S. Dhakar, A. Parui, P. Gakhad, A.K. Singh, K. Biswas, C.S. Tiwary, and S. Sharma, "Electrooxidation of hydrazine utilizing high-entropy alloys: assisting the oxygen evolution reaction at the thermodynamic voltage," ACS Catalysis, vol. 11, no. 22, pp.14000-14007, 2021.

[17] K. Li, and W. Chen, "Recent progress in high-entropy alloys for catalysts: synthesis, applications, and prospects," Materials Today Energy, vol. 20, pp.100638, 2021.

[18] H. Wang, R. Wei, X. Li, X. Ma, X. Hao, and G. "Guan, Nanostructured amorphous Fe29Co27Ni23Si9B12 high-entropy-alloy: an efficient electrocatalyst for oxygen evolution reaction," Journal of Materials Science & Technology, vol. 68, pp.191-198, 2021.

[19] A. Komathi, M. Pushpa Rani, "Shift reduce parser based malicious sensor detection for predicting forest fire in WSNs," Wireless Personal Communications, vol. 103, pp. 2843-2861, 2018.

[20] P. Zhou, D. Liu, Y. Chen, M. Chen, Y. Liu, S. Chen, C.T. Kwok, Y. Tang, S. Wang, and H. Pan, "Corrosion engineering boosting bulk Fe50Mn30Co10Cr10 high-entropy alloy as high-efficient alkaline oxygen evolution reaction electrocatalyst," Journal of Materials Science & Technology, vol. 109, pp.267-275, 2022.

[21] Nihar Ranjan Kar, "A Review on Targeting of Drugs to Brain," Indian Journal of Natural Sciences, vol. 11, no. 64, 2021.

[22] K. Huang, B. Zhang, J. Wu, T. Zhang, D. Peng, X. Cao, Z. Zhang, Z. Li, and Y. Huang, "Exploring the impact of atomic lattice deformation on oxygen evolution reactions based on a sub-5 nm pure face-centred cubic high-entropy alloy electrocatalyst," Journal of Materials Chemistry A, vol. 8, no. 24, pp.11938-11947, 2020.

[23] Z. Lu, Z.W. Chen, and C.V. Singh, "Neural network-assisted development of high-entropy alloy catalysts: Decoupling ligand and coordination effects," Matter, vol. 3, no. 4, pp.1318-1333, 2020.

[24] N. Mary Peter, M, Pushpa Rani, "V2V communication and authentication: the internet of things vehicles (IoTV)," Wireless Personal Communications, vol.120, no.1, pp. 231-247, 2021.

[25] X. Wan, Z. Zhang, W. Yu, H. Niu, X. Wang, and Y. Guo, "Machine-learning-assisted discovery of highly efficient high-entropy alloy catalysts for the oxygen reduction reaction," Patterns, pp.100553, 2022.

[26] L. Fan, Y. Ji, G. Wang, J. Chen, K. Chen, X. Liu, and Z. Wen, "High Entropy Alloy Electrocatalytic Electrode toward Alkaline Glycerol Valorization Coupling with Acidic Hydrogen Production," Journal of the American Chemical Society, vol. 144, no. 16, pp.7224-7235, 2022.

[27] H. Chen, C. Guan, and H. Feng, "Pt-Based High-Entropy Alloy Nanoparticles as Bifunctional Electrocatalysts for Hydrogen and Oxygen Evolution," ACS Applied Nano Materials, vol. 5, no. 7, pp.9810-9817, 2022.

[28] P. Brinda, M. Pushpa Rani, "Analysis of Early Leave Pest Detection," International Journal on Recent and Innovation Trends in Computing and Communication, vol. 4, no.5, pp. 2321-8169, 2016.

[29] C.M. Clausen, M.L.S. Nielsen, J.K. Pedersen, and J. Rossmeisl, "Ab Initio to activity: Machine learning assisted optimization of high-entropy alloy catalytic activity," 2022.

[30] Y. Mei, Y. Feng, C. Zhang, Y. Zhang, Q. Qi, and J. Hu, "High-Entropy Alloy with Mo-Coordination as Efficient Electrocatalyst for Oxygen Evolution Reaction," ACS Catalysis, vol. 12, pp.10808-10817, 2022.

[31] L. Sharma, N.K. Katiyar, A. Parui, R. Das, R. Kumar, C.S. Tiwary, A.K. Singh, A. Halder, and K. Biswas, "Low-cost high entropy alloy (HEA) for high-efficiency oxygen evolution reaction (OER)," Nano Research, vol. 15, no. 6, pp.4799-4806, 2022.

[32] P. Li, X. Wan, J. Su, W. Liu, Y. Guo, H. Yin, and D. Wang, "A Single-Phase FeCoNiMnMo High-Entropy Alloy Oxygen Evolution Anode Working in Alkaline Solution for over 1000 h," ACS Catalysis, vol. 12, pp.11667-11674, 2022.

[33] S. Wang, W. Huo, F. Fang, Z. Xie, J.K. Shang, and J. Jiang, "High entropy alloy/C nanoparticles derived from polymetallic MOF as promising electrocatalysts for alkaline oxygen evolution reaction," Chemical Engineering Journal, vol. 429, pp.132410, 2022.

[34] Y. Mei, Y. Feng, C. Zhang, Y. Zhang, Q. Qi, and J. Hu, "High-Entropy Alloy with Mo-Coordination as Efficient Electrocatalyst for Oxygen Evolution Reaction," ACS Catalysis, vol. 12, pp.10808-10817, 2022.

[35] L. Zhang, W. Ji, J. Gu, Q. Jiang, K. Liu, M. Huang, P. Liu, P. Ma, and Z. Fu, "Construction of metal (oxy) hydroxides surface on high entropy alloy as lattice-oxygen-participated electrocatalyst for oxygen evolution reaction," Journal of Electroanalytical Chemistry, vol. 920, pp.116574, 2022.

[36] A.P. Senthil Kumar, S. Yuvaraj, S. Janaki, "Experimental investigations of Co3O4, SiO2, cotton seed oil additive blends in the diesel engine and optimization by ANN-SVM process," Journal of Ceramic Processing Research, vol. 21, no. 2, pp. 217-225, 2020.

[37] S. Yuvaraj, A.P. Senthil Kumar, M. Muthukumar, K. Sadesh, S. Janaki, "Certain studies on influence of nano catalysts Co3O4, SiO2 blended with CME-diesel in combustion," Materials Today: Proceedings, vol. 51, pp. 1612-1618, 2022.

[38] Tarun Kumar Kotteda, Manoj Kumar, Pramod Kumar, Rama Bhadri Raju Chekuri, "Metal matrix nanocomposites: future scope in the fabrication and machining techniques," The International Journal of Advanced Manufacturing Technology, 2022. https://doi.org/10.1007/s00170-022-09847-0

[39] Tarun Kumar Kotteda, Rama Bhadri Raju Chekuri, Naga Raju, Prasada Raju Kantheti, S. Balakumar, "Analysis on Emissions and Performance of Ceramic Coated Diesel Engine Fueled with Novel Blends Using Artificial Intelligence," Advances in Materials Science and Engineering, 2021, https://doi.org/10.1155/2021/7954488

[40] R.K. Pattanaik, S. Mishra, M. Siddique, T. Gopikrishna, S. Satapathy, "Breast Cancer Classification from Mammogram Images Using Extreme Learning Machine-Based DenseNet121 Model," Genetics Research, pp. 2731364, 2022.

[41] S.K. Mohapatra, S. Prasad, G.M. Habtemariam, M. Siddique, "Identify determinants of infant and child mortality based using machine learning: Case study on Ethiopia," Big Data Analytics and Machine Intelligence in Biomedical and Health Informatics: Concepts, Methodologies, Tools and Applications, pp. 21–45, 2022.

[42] M. Siddique, D. Panda, "Prediction of stock index of tata steel using hybrid machine learning based optimization techniques," International Journal of Recent Technology and Engineering, vol. 8, no. 2, pp. 3186–3193, 2019.

[43] M. Siddique, D. Panda, "A hybrid forecasting model for prediction of stock index of tata motors using principal component analysis, support vector regression and particle swarm optimization," International Journal of Engineering and Advanced Technology, vol. 9, no. 1, pp. 3032–3037, 2019.

[44] S. S. Reddy, N. Sethi, R. Rajender, & V.S.R. Vetukuri, "Non-invasive diagnosis of diabetes using chaotic features and genetic learning," In Third International Conference on Image Processing and Capsule Networks, pp. 161–170, 2022. Cham: Springer International Publishing.

[45] S. S. Reddy, L. Alluri, M. Gadiraju, & R. Devareddi, "Forecasting Diabetic Foot Ulcers Using Deep Learning Models," Proceedings of Third International Conference on Sustainable Expert Systems, pp 211–227, 2023.

[46] R. S. Shankar, D. R. Babu, K.V.S.S. Murthy, & V. Gupta, 'An approach for essay evaluation using system tools," 2017 International Conference on Innovative Research In Electrical Sciences (IICIRES). IEEE. 2017.

[47] R. Shiva Shankar, & D. Ravibabu, "Digital report grading using NLP feature selection," In Soft Computing in Data Analytics,615–623, 2019. Proceedings of International Conference on SCDA 2018.

[48] Reddy, Shiva Shankar, M. Gadiraju, & V.V.R. Maheswara Rao, "Analyzing student reviews on teacher performance using long short-term memory," In Innovative Data Communication Technologies and Application, pp. 539–553, 2022. Singapore: Springer Nature Singapore.